Proceedings of the IX Bulgarian-Serbian Astronomical Conference: Astroinformatics (IX BSACA) Sofia, Bulgaria, July 2-4, 2014,
Editors: M. K. Tsvetkov, M. S. Dimitrijević, O. Kounchev, D. Jevremović and K. Tsvetkova
Publ. Astron. Soc. "Rudjer Bošković" No 15, 2015, 75-82

BROAD SPECTRAL LINE AND CONTINUUM VARIABILITIES IN QSO SPECTRA INDUCED BY MICROLENSING:METHODS OF COMPUTATION

SAŠA SIMIĆ[1] and LUKA Č. POPOVIĆ[2]

[1]*Faculty of Science, Department of Physics, University of Kragujevac*
E-mail: ssimic@kg.ac.rs
[2]*Astronomical Observatory Belgrade, Serbia*
E-mail: lpopovic@aob.rs

Abstract. We present methods and algorithms for computation of magnification maps and images of source in the case of microlensed QSO. The source (QSO) is assumed to be complex, that emits the continuum from an accretion disk and H_β broad line from the Broad Line Region (BLR). Accretion disk is assumed to be a standard, geometrically thin, optically thick, while BLR region is uniformly distributed around the disk with much larger diameter. Here we present the computational methodology for calculation of variability of H_β line during the crossing. This computation can be easily applied to the more complicated objects, like AGNs with binary black hole system. We present the results of spectral line variability during the full rotational period for binary system.

1. INTRODUCTION

Deflection of light while passing close to the massive astronomical objects is old and well established problem. In short, photons of light while crossing a certain distance follow the geodesics of space-time which are curved in the close vicinity of a massive object. The amount of deviation from straight line directly depends on the distribution of the interacting mass. This view has been considered exactly by Einstein in his work on General theory of Relativity, producing the rather simple solution, for deflection angle in case of a point like source and lens:

$$\alpha = \frac{4GM}{c^2 R}, \tag{1}$$

where R is the impact parameter, M mass of the lens and G and c are gravitational and light speed constant. In a simple case scenario, of point source and one perfectly spherical deflector (see Fig. 1), it is easy to compute paths of the light rays and deflection angle, by using the Eq. 1.

However, in other more realistic cases which for example include lens containing a number of randomly distributed deflector objects (usually the stars) or extended

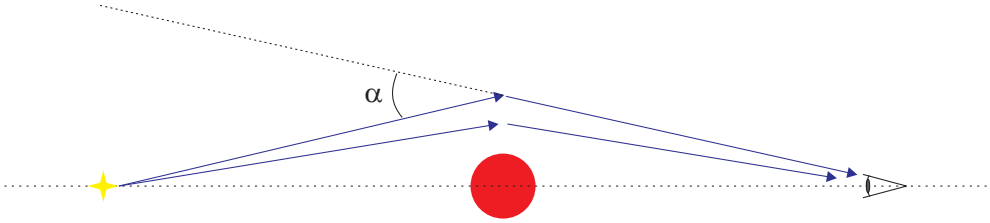

Figure 1: The point-like source presented at left side (yellow colored star) and deflector as a point-like massive object in the middle (red circle). Observer detect the deflected radiation.

instead of the point like source, those computations are rather complicated and more computer time consuming. In those cases one must implement suitable algorithms for computing the trajectories of light rays from all parts of the source, which are deflected by the complex lens structure, toward the observer.

In the case of a point like source those algorithms are discussed in details by Paczynski (1986), Kayser, et al. (1986), Schneider and Weiss (1986, 1987), and for the case of extended source by Treyer and Wambsganss (2004). They have used ray shooting technique to determine the path of light rays and in case of Treyer and Wambsganss (2004), convolution for computing the light curves of magnified sources. On the basis of their work we have applied these methods on the complex extended source with specific Spectral Energy Distribution (SED) and appropriate spectral lines. We have also avoid to use convolution for computing the light curves of source, but instead sum all contribution of particular pixels in the total emission output.

In the Chapters §2 and §3 we presented the computational model used together with our modifications, and in the Chapter §4 we present the results.

2. METHODS OF COMPUTATION

To calculate the microlensing of a distante source one needs to follow the rays of light from each part of the source toward the lens and observer plane. This is called ray-tracing method and it is highly computational demanding, since all possible paths of light rays have to be followed. On the other hand if we assume that observer can see only rays which fall in it's point, than the overall number of followed light-rays can be significantly reduced. This as a result substantially reduce the needed computational time. Therefore, we follow the rays of light in opposite direction, from the observer point toward the lens plane and further on the source plane (see Fig. 2). This is called the ray shooting method.

As one can see in Fig. 2 light rays are directed from the observer point uniformly toward the lens plane, where a certain number of point-like Solar mass deflectors are uniformly distributed. They produce a cumulative effect on the passing rays which can be accounted by computing the overall gravitational potential and consequently lensing potential. Knowing the lensing potential it is easy to compute deflection angle for particular light ray and further more a point in the source plane where this light ray will fall. For a great number of light rays shooted from the observer and deflected

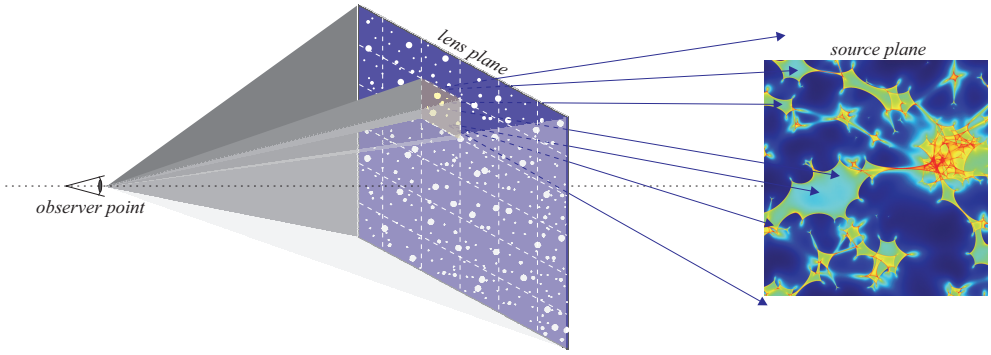

Figure 2: Scheme of ray shooting mehtod (see text).

by lens a collection in the source plane will be created, so called the magnification map. It presents a distribution of light rays deflected by lens, over the pixel map created in the source plane, which can be seen by the observer (see Fig. 2). When a light ray falls on the particular pixel in the source plane then it is accounted by summing with rest of the rays fallen on the same pixel. For better presentation we use rainbow color coding system, which means that for those pixels who collect more light rays, the lighter color is used, usually yellow or red, but if the number of fallen rays is lower, than color coding is green or blue.

Magnification map alone, does not present a source of light and can not be seen by an observer. Rather it gives a distribution of the amount of magnification each pixel can impose on fictional source itself. If we place the extend source on the same grid where magnification map is spread, then their superposition is calculated by multiplying the magnification of particular pixel with the intensity generated by the source at the position of pixel. At the end the result is achieved when we trace back magnified light rays toward the grid in the lens plane in order to create lensed image of the source.

Practical work with this method regards, first to divide the lens plane into segments (as shown on the Figure 1), then to compute the gravitational and lensing potential for each cell. In the source plane we construct a matrix of pixels which collect the light rays deflected by lens. Depending on the source dimension, usually we choose that source matrix has dimension of 2000 by 2000 pixels, dimension of the lens plane is about 10 times higher, and number of lens segments is mostly 256 or 512 pixels. Also, for constructing the source image in the lens plane we setup a matrix with same dimensions as for the source.

3. PARAMETERS OF SOURCE AND LENS

To apply described method we consider the complex source and lens. Here we will consider as a source an Active Galactic Nucleus (AGN) that has wavelength dependent structure. This practically means that different parts have emission in different spectral bands, i.e. a wavelength dependent emission of different regions are present in AGNs (see e.g. Popović et al. 2012). It is widely accepted that the majority

of radiation is coming from the accelerated material spiraling down toward the black hole in a form of an accretion disc. The radiation from the disc is mostly thermalized from outer regions R_{out} to the center, with slight exception at inner radius, i.e. very close to the black hole, where Compton upscattering due to the high mass accretion could have a significant role (see Done et al. 2012, Popović and Simić, 2014, Simić and Popović, 2014a). The disc inclination can be changed, but in the most simulations we assumed a face-on disc orientation.

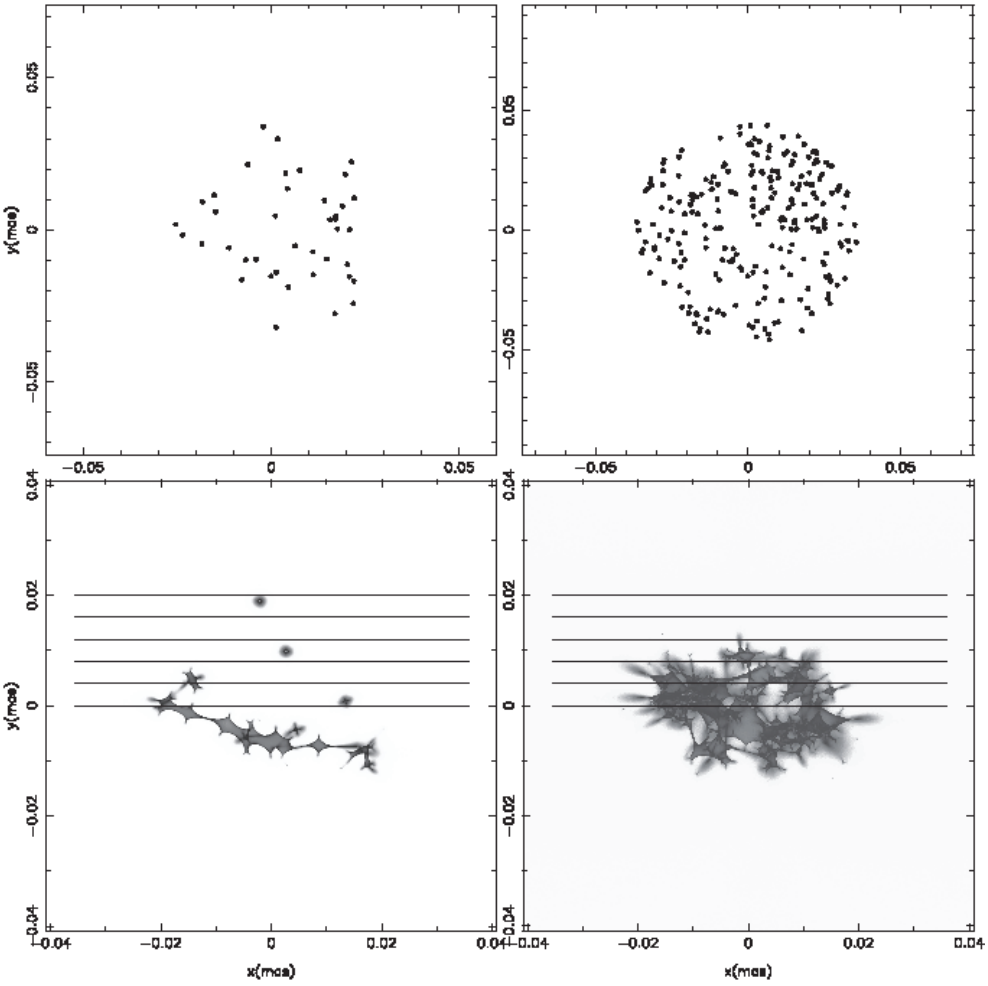

Figure 3: Upper panels show a random star distribution in the lens plane, a) case of $n_{lens} = 40$ (left panels) and b) case for $n_{lens} = 240$ (right panels). In the bottom panels we give the appropriate magnification map in the source plane for specified n_{lens}, respectively. Horizontal parallel solid lines present the paths of the source for which we calculated magnification light curves and variability of the photo-center positions. These plots are given for a standard lens system with $z_d = 0.5$ and $z_s = 2.0$ (Popović and Simić, 2014).

The lens has been assumed to have a circular shape, containing N_s stars of Solar masses ranging from 40 to 240 in this particular case, see Figure 3. We also assumed that lens and source are placed at the cosmological distances, with $z_d = 0.5$ and $z_s = 2.0$ (standard lens). We are confident that such carefully chosen lens reflects good enough condition for the gravitational bound systems. Any more massive and densely populated lens will act as one compact object with known influence on the distant source.

4. RESULTS

By using ray shooting method we are able to investigate effects of microlens on the observed AGN source. In the first place we present the lens with appropriate magnification maps and images of AGN perturbed by microlensing of a diffuse massive structure. In Figure 3 one can see the distribution of stars in the lens for two discussed cases, together with their respectfull magnification maps. As it is expected in case of higher populated lenses more caustics are distributed in the magnification maps. This case then have similar influence as one compact lens with similar mass. For lower populated lenses the perturbation of source light curve has more iregular impact with highly expressed peaks.

In the Figure 4 we can see that depending on the number of stars in the lens, image can become more or less deviated. In both cases we consider uniform distribution of stars in the lens as presented in the Figure 2. It is well known that AGN have particular SED which significantly depends on wavelengths, we compute the images in four different spectral bands. In both cases of lens population, we can see that images in lower energy bands are bigger then in higher energy bands.

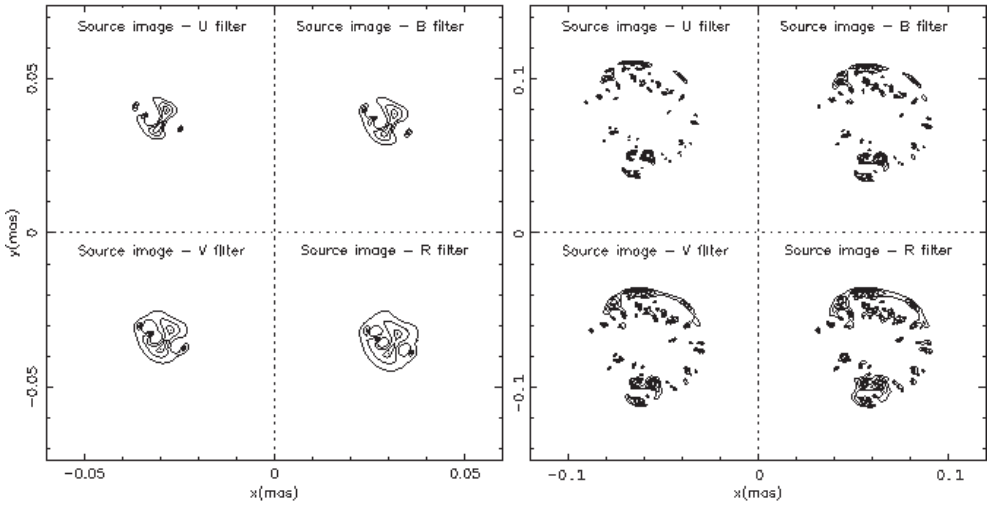

Figure 4: Images of source in four different energy channels U[332-398 nm], B[398-492 nm], V[507-595 nm] and R[589-727 nm]. Lens for this case is presented in Figure 3. Left four panels present the image for the case of $n_{lens} = 40$, while four on the right side are for the $n_{lens} = 240$ stars, with $z_d = 0.5$ and $z_s = 2.0$.

Additionally, by knowing the emission distribution over pixels of the AGN image, we compute light curve variations induced by crossing of lens over an AGN source, for both cases of lens population, see Fig. 5.

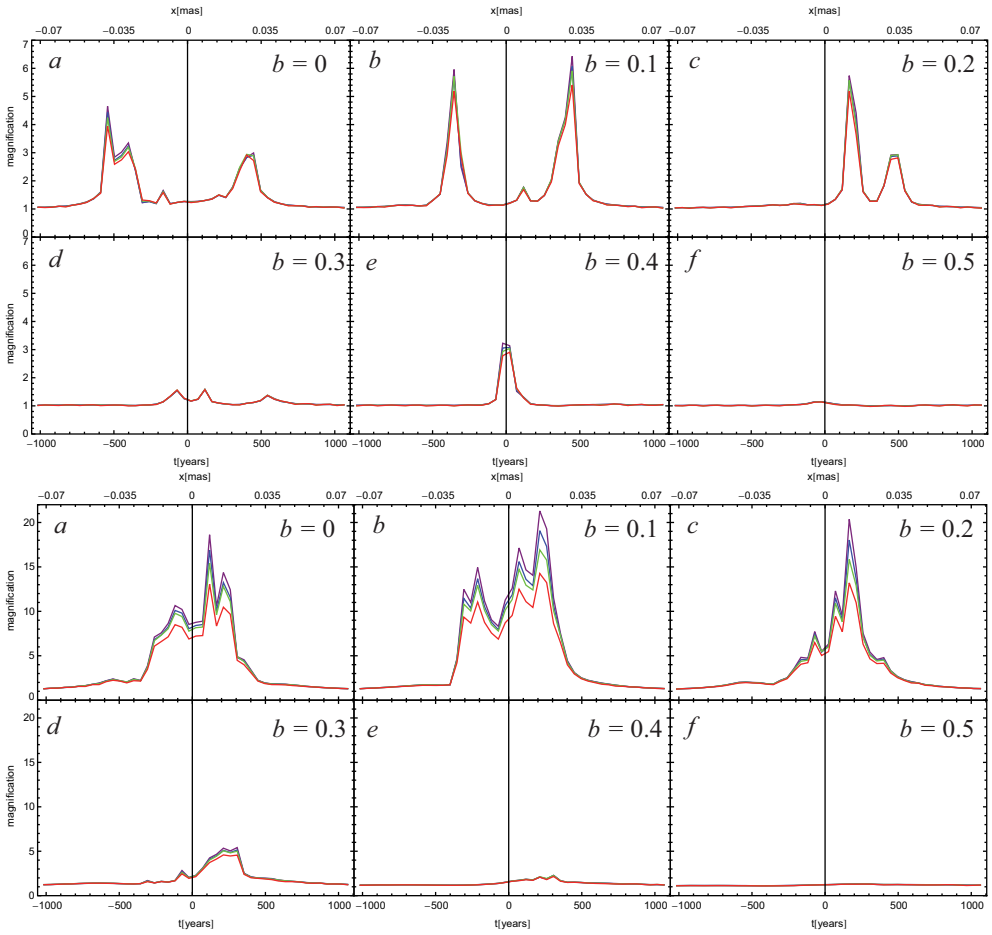

Figure 5: Magnification variability of a source image during the overcrossing event. Lens is populated with 40 and 240 Solar mass stars distributed uniformly in the circular area. In panels from a) to f) (upper and lower image) impact parameter b changes from 0 towards maximum value equal to the half of the half height of source map. Trajectories are presented as in the Figure 4.

We shell point out here that one peak in light curves presents a variation caused by a single caustic in the map (caused by a group of stars), with relative variation as much as 5 to 7 times. On the contrary, in the second case (Fig. 5), with a more massive lens (240 stars) we have the proportionally higher relative magnification of the order of 20 times, caused by an action of a bulk of overlapping caustics which gradually decreases with an increase of parameter b. For the last two cases e) and f)

in Fig. 5 the magnification is neglected. Such behavior suggests that the lens acts as a compact object with the mass equal to the sum of masses of all stars in the cluster. In both cases relative deviations per observed energy channels is at maximum for the moment of the highest magnification with the maximum in the U channel and decreased for another channels.

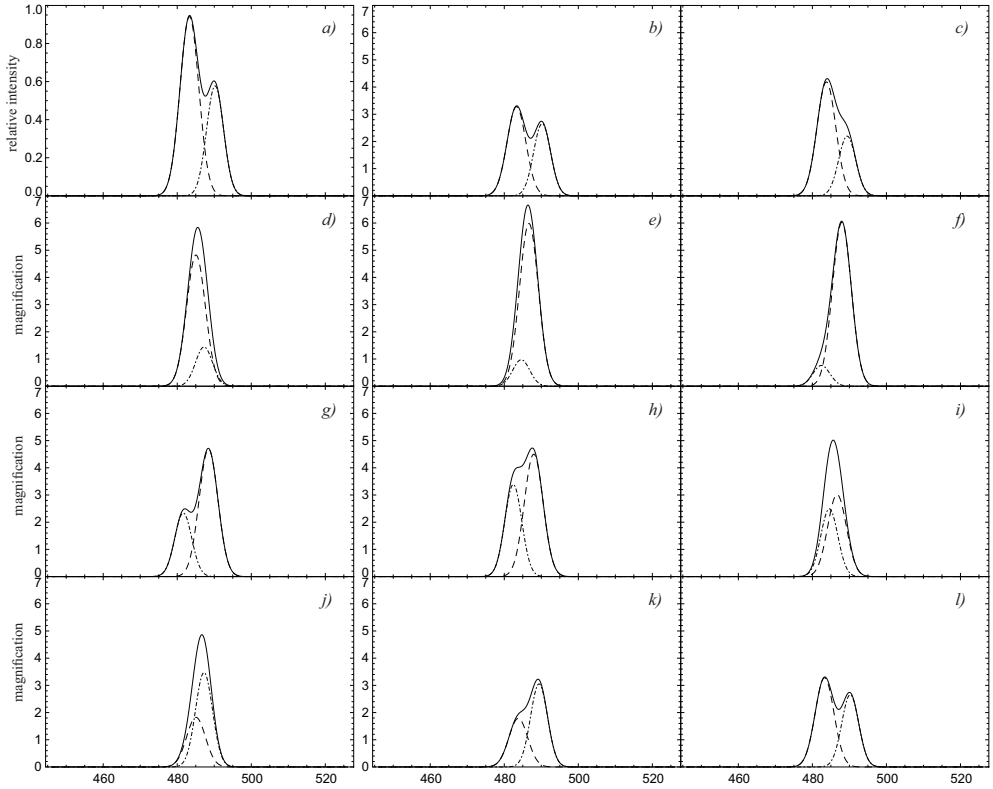

Figure 6: H_β spectral line from the binary system of super massive binary black holes, influenced by microlens during the full rotation. First image a) is without microlens with unit magnification. Dashed and dotted lines presents H_β spectral line for particular binary component, while full line presents their superposition.

In the case of a super massive binary black hole system (SMBBH) we have applied the presented method for computing the magnification maps and images (Simić and Popović, 2014a, in preparation). As most interesting we present the variability induced by microlens action on the H_β spectral line, during the full rotation of the system (see Fig. 6). It is very interesting to note that microlens can magnify or demagnify component lines, which has significant influence in composite line profile. One can see that magnification of both lines can be as high as 7 times in comparision with unlensed system.

5. CONCLUSION

In this paper we have presented the methodology used for computation of microlens influence on the distant source, particulary the AGNs. We have showed that the ray shooting algorithm is more efficient than the ray tracing method. We have presented a method and apply it in the case of a complex source (AGN) and taking a complex lens (massive diffusive object).

We found that presented method can be applied for a vast number of different cases. What is important to express is that applied method allow us to exactly follow each of the possible light rays emitted from the source and precisely determine deflection induced by lens. We additionally upgrade method by introducing the spectral stratification of particular pixels contained in source. This allows to study even spectral behavior of source under the microlensing influence.

Acknowledgments

This work is a part of the project (176001) *Astrophysical Spectroscopy of Extragalactic Objects*, supported by the Ministry of Science and Technological Development of Serbia.

References

Done C., Davis, S.W., Jin, C, Blaes, O., Ward, M.: 2012, Intristic disc emission and the soft X-ray excess in active galactic nuclei, *MNRAS*, **420**, 1848.

Kayser, R., Refsdal, S., Stabell, R.: 1986, Astrophysical applications of gravitational microlensing, *A&A*, **166**, 36.

Paczynski, B.: 1986, Gravitational microlensing at large optical depth, *ApJ*, **301**, 503.

Popović, L. Č., Jovanović, P., Stalevski, M., Anton, S., Andrei, A. H., Kovačević, J., Baes, M.: 2012, Photocentric variability of quasars caused by variation in their innner structure: consequence for Gaia measurements, *A&A*, **538A**, 107.

Popović, L. Č., Simić, S.: 2013, Spectro-photometric variability of quasars, caused by lensing of diffuse massive substructure: consequence on flux anomaly and precise astrometric measurements, *MNRAS*, **432**, 848.

Simić, S. & Popović, L. Č.: 2014, Broad spectral line and continuum variabilities in QSO spectra induced by microlensing of diffusive massive substructure, *ASR*, **54**, 1439.

Simić, S. & Popović, L. Č.: 2014a, in preparation.

Schneider, P. & Weiss, A.: 1986, The two-point-mass lens: detailed investigation of a special asymmetric gravitational lens, *A&A*, **164**, 237.

Schneider, P. & Weiss, A.: 1987, A gravitational lens origin for AGN-variability? Consequence of micro-lensing, *A&A*, **171**, 49.

Treyer, M. & Wambsganss, J.: 2004, Astrometric microlensing of quasars. Dependence on surface mass density and external shear, *A&A*, **416**, 19.